IAI Journals.ASM.org

Porphyromonas gingivalis Infection-Associated Periodontal Bone Resorption Is Dependent on Receptor Activator of NF-κB Ligand

Xiaozhe Han,[a] Xiaoping Lin,[a,b] Xiaoqian Yu,[a,c] Jiang Lin,[a,d] Toshihisa Kawai,[a] Karen B. LaRosa,[a] Martin A. Taubman[a]

Department of Immunology and Infectious Diseases, The Forsyth Institute, Cambridge, Massachusetts, USA[a]; Department of Stomatology, Shengjing Hospital of China Medical University, Shenyang, Liaoning Province, China[b]; Department of Periodontology, Peking University School of Stomatology and Hospital of Stomatology, Beijing, China[c]; Department of Stomatology, Fourth College of Harbin Medical University, Harbin, China[d]

***Porphyromonas gingivalis* is one of the oral microorganisms associated with human chronic periodontitis. The purpose of this study is to determine the role of the receptor activator of nuclear factor-κB ligand (RANKL) in *P. gingivalis* infection-associated periodontal bone resorption. Inbred female Rowett rats were infected orally on four consecutive days (days 0 to 3) with 1×10^9 *P. gingivalis* bacteria (strain ATCC 33277). Separate groups of rats also received an injection of anti-RANKL antibody, osteoprotegerin fusion protein (OPG-Fc), or a control fusion protein (L6-Fc) into gingival papillae in addition to *P. gingivalis* infection. Robust serum IgG and salivary IgA antibody ($P < 0.01$) and T cell proliferation ($P < 0.05$) responses to *P. gingivalis* were detected at day 7 and peaked at day 28 in *P. gingivalis*-infected rats. Both the concentration of soluble RANKL (sRANKL) in rat gingival tissues ($P < 0.01$) and periodontal bone resorption ($P < 0.05$) were significantly elevated at day 28 in the *P. gingivalis*-infected group compared to levels in the uninfected group. Correspondingly, RANKL-expressing T and B cells in rat gingival tissues were significantly increased at day 28 in the *P. gingivalis*-infected group compared to the levels in the uninfected group ($P < 0.01$). Injection of anti-RANKL antibody ($P < 0.05$) or OPG-Fc ($P < 0.01$), but not L6-Fc, into rat gingival papillae after *P. gingivalis* infection resulted in significantly reduced periodontal bone resorption. This study suggests that *P. gingivalis* infection-associated periodontal bone resorption is RANKL dependent and is accompanied by increased local infiltration of RANKL-expressing T and B cells.**

Periodontitis is an inflammatory disease triggered by the host immune response to a constellation of periodontal biofilm-associated microorganisms (1–4). Intervening between the infection site and the targets of the disease (bone and connective tissue) is a dense mononuclear inflammatory infiltrate containing all cellular components necessary to control immunologically interactive networks. Abundant T and B lymphocytes are found in this infiltrate, and these inflammatory cells can infiltrate gingival tissues in an antigen-specific manner (1, 5, 6). A key finding in previous studies is the presence of abundant osteoclasts on the alveolar bone (AvB) crest of the animals receiving antigen-specific lymphocytes, strongly implicating the immune response in the induction of bone resorption (1, 5).

Recently, a close relationship between the immune and skeletal systems has attracted much attention due to accumulating evidence that bone destruction can be caused by an inflammatory activation of the immune system in rheumatoid arthritis (7–9) and in periodontitis (1, 10, 11). Receptor activator of NF-κB ligand (RANKL) is a tumor necrosis factor (TNF)-related cytokine that has been reported to be involved in not only physiological osteoclastogenesis but also pathological bone resorption (12–14). RANKL has been shown to be expressed not only in osteoblasts and bone marrow stromal cells but also in T cells and B cells (15–17), indicating that RANKL is a requisite factor for the initiation of osteoclastogenesis in pathogenic bone resorption lesions as well as in homeostatic bone remodeling. Importantly, our studies involving immunohistochemical analyses and confocal microscopy of the periodontal lesions indicated abundant RANKL expression on T and B cells, with little or no expression of RANKL by macrophages of patients with chronic periodontitis (18).

In the rat adoptive transfer/gingival challenge model of periodontitis, we have demonstrated that periodontal bone resorption is associated with increased expression and activity of RANKL by infiltrating, antigen-specific T and B cells and subsequent induction of osteoclastogenesis (1, 5, 19). Other investigators with similar models have obtained comparable results (20, 21). In this study, we developed an experimental model of rat periodontal disease by infection with *Porphyromonas gingivalis*, a Gram-negative anaerobic bacterium that has been associated with the development of periodontal disease, and investigated the role of immune cell RANKL expression in periodontal bone resorption in this model.

MATERIALS AND METHODS

Rat oral infection with *P. gingivalis*. All animals were inbred female Rowett rats ($Rnu^{/+}$; 2 to 3 month old) maintained under pathogen-free conditions in laminar flow cabinets. Experiments using these animals were approved by the Forsyth Institute's Internal Animal Care and Use Committee (IACUC). In experiment 1, 36 animals were randomly divided into a control group (18 animals) and an infection group (18 animals). For the infection group, rats were orally infected with live *Porphyromonas gingivalis* bacteria (ATCC 33277). *P. gingivalis* was grown in Trypticase soy broth (BD Biosciences, San Diego, CA) containing 1% yeast extract, 5 μg/ml hemin, and 2.5 μg/ml menadione as previously described (22). Bacteria number in culture broth was determined by reading absorbance values using a spectrophotometer and comparing values

Received 10 January 2013 **Accepted** 14 February 2013
Published ahead of print 25 February 2013
Editor: S. R. Blanke
Address correspondence to Xiaozhe Han, xhan@forsyth.org.

doi:10.1128/IAI.00043-13

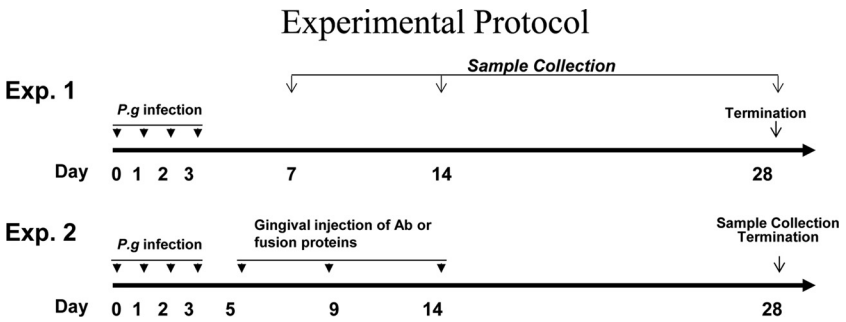

FIG 1 Summary of experimental protocol. For experiment (Exp) 1, 36 animals were randomly divided into a control group (18 animals) and an infection group (18 animals), and after four consecutive days of infection, serum, saliva, cervical LN, and gingival samples from each animal were collected at days 7, 14, and 28 ($n = 6$ for each time point). For experiment 2, 40 animals were randomly divided into five groups (control, infection only, infection plus anti-RANKL IgG, infection plus OPG-Fc, and infection plus L6-Fc; $n = 8$ for each group). Samples were collected on day 28 after different treatments. For each group, gingival tissues and maxillae were collected from four animals, and another four animals were used for histological analyses. Ab, antibody; *P. g.*, *P. gingivalis*.

to a curve derived from a standard plate count. The infection was administered by oral gavage using 10^9 *P. gingivalis* bacteria per animal per day for four consecutive days (days 0 to 3). Briefly, an equal volume of sterile 2% (wt/vol) low-viscosity carboxymethylcellulose (CMC) was added and mixed thoroughly, and 1 ml of *P. gingivalis* culture was administered by oral gavage. The uninfected group was used as a control. Animals were sacrificed, and samples (serum, saliva, cervical lymph nodes [LN], and gingivae) were collected at days 7, 14, and 28 ($n = 6$ for each time point). In experiment 2, 40 animals were randomly distributed into the following five groups ($n = 8$ per group): group 1, control uninfected; group 2, *P. gingivalis* infection only; group 3, *P. gingivalis* infection and gingival injection of anti-RANKL (xRANKL) IgG antibody (1 μg/site); group 4, *P. gingivalis* infection and gingival injection of human osteoprotegerin fusion protein (OPG-Fc; 0.5 μg/site); or group 5, *P. gingivalis* infection and gingival injection of a control fusion protein (L6-Fc; 0.5 μg/site). Each rat received three palatal gingival injections (1 μl/site) on the mesial of the first molar and in the papillae between molars on both sides (three sites on each side) of the maxilla using a 28.5-gauge double-beveled MicroFine needle (Becton, Dickinson). The injections for animals in groups 3 to 5 were administered into rat palatal gingival papillae three times (day 5, day 9, and day 14). Experiments were terminated at day 28. A summary of the experimental protocol is shown in Fig. 1.

ELISA. Rat serum and saliva samples were collected as previously described (22). Formalin-fixed *P. gingivalis* bacteria (10^7 bacteria/well) were coated onto 96-well plates. For the detection of serum IgG antibody to *P. gingivalis* ($n = 6$), diluted rat serum (1:500) was applied to the plate, and rabbit (Rb) anti-rat IgG antibody was added, followed by alkaline phosphatase (ALP)-conjugated goat anti-rabbit IgG antibody (Sigma). For the detection of salivary IgA antibody to *P. gingivalis* ($n = 6$), diluted rat whole saliva (1:20) was applied to the plate, and mouse anti-rat IgA antibody (Biosource International, Camarillo, CA) was added, followed by ALP-conjugated goat anti-mouse IgG antibody (Sigma). Colorimetric reactions were developed with *p*-nitrophenyl phosphate (pNPP) substrate and measured at 405 nm using a spectrophotometer (Biotek, Winooski, VT). Enzyme-linked immunosorbent assay (ELISA) measurements were performed, and results are expressed as ELISA units (EU) based on a reference curve provided by dilution of an antibody-containing hyperimmune rat serum collected from rats immunized with *P. gingivalis* (18). Gingival tissues were homogenized with a Dounce glass homogenizer in phosphate-buffered saline (PBS) with 0.05% Tween 20, phenylmethylsulfonyl fluoride (Sigma), and proteinase inhibitor cocktail (Sigma) as described previously (5). The quantitation of soluble RANKL (sRANKL) in rat gingival homogenates ($n = 6$) was assayed in triplicate using a murine sRANKL ELISA development kit (Peprotech), and the concentration (pg/ml) of soluble RANKL in each sample was calculated from a standard curve.

T cell proliferation assay. Immune cells from rat cervical lymph nodes ($n = 6$) were isolated and cultured in 96-well plates (1×10^4 cells/well) in triplicate in the presence of formalin-fixed *P. gingivalis* (1×10^7 bacteria/well). [^{3}H]thymidine (0.5 μCi/well) was added for the last 16 h of a 4-day culture. Samples were harvested onto glass fiber filters, and radioactivity (cpm) was measured in a liquid scintillation spectrometer (PerkinElmer, Waltham, MA).

Flow cytometry. Mononuclear cells were isolated from rat gingival tissues ($n = 4$) as described previously (19) and stained with the following monoclonal mouse anti-rat antibodies (AbD Serotec, Oxford, United Kingdom): OX33 (B cells), R73 (T cells), NK-RP1 (natural killer cells), and ED1 (macrophages). After cells were washed with PBS, they were stained with fluorescein isothiocyanate (FITC)-conjugated rat anti-mouse IgG (Jackson ImmunoResearch). For the detection of membrane RANKL expression, cells were also stained with rabbit anti-RANKL IgG followed with phycoerythrin (PE)-conjugated goat anti-rabbit IgG (Molecular probes). FITC-conjugated mouse and rabbit IgG isotype controls (AbD Serotec, Oxford, United Kingdom) were used as negative controls. The number of positively stained cells in the total counted cells (20,000) was analyzed for each sample using an Epics Altra flow cytometer (Beckman Coulter).

TRAP assay. The mouse macrophage/monocyte cell line RAW 264.7 (ATCC TIB-71) was seeded in 96-well plates at a density of 10^3 cells/well in 10% fetal bovine serum (FBS) containing Dulbecco's modified Eagle's medium (DMEM). RAW 264.7 cells were cultured for 5 days with 50 ng/ml murine recombinant RANKL (mrRANKL; R&D Systems) in the presence or absence of rabbit (Rb) normal serum IgG or Rb anti-RANKL IgG. In some experiments, RAW 264.7 cells were cultured for 2 days with mrRANKL (50 ng/ml). Then the medium was replaced with fresh medium without mrRANKL, and cells were cultured with rat gingival homogenates ($n = 4$) (0.25 μg/ml or 2.5 μg/ml) for another 3 days in the presence or absence of anti-RANKL IgG (1 μg/ml, 5 μg/ml, or 10 μg/ml). Cells were stained for tartrate-resistant acid phosphatase (TRAP) using a leukocyte acid phosphatase kit (Sigma) as previously described (1). TRAP-positive(TRAP$^+$) cells with three or more nuclei were considered osteoclasts. TRAP$^+$ multinuclear cells were counted, and results are expressed as numbers per well in a 96-well plate.

Measurement of alveolar bone resorption. After defleshing of the maxillary jaws, periodontal bone resorption was measured as previously described (1). Briefly, the distances from cemento-enamel junction (CEJ) to the alveolar bone (AvB) crest on the palatal side of each root were measured using a microscope with a reticule eyepiece under ×25 magnification. Recordings were made in the long axis of the root surfaces of all molar teeth. A total of 14 recordings were evaluated in each rat, including three roots of the first molar and both roots of the second and the third molars. Measurements were made by an examiner without prior knowl-

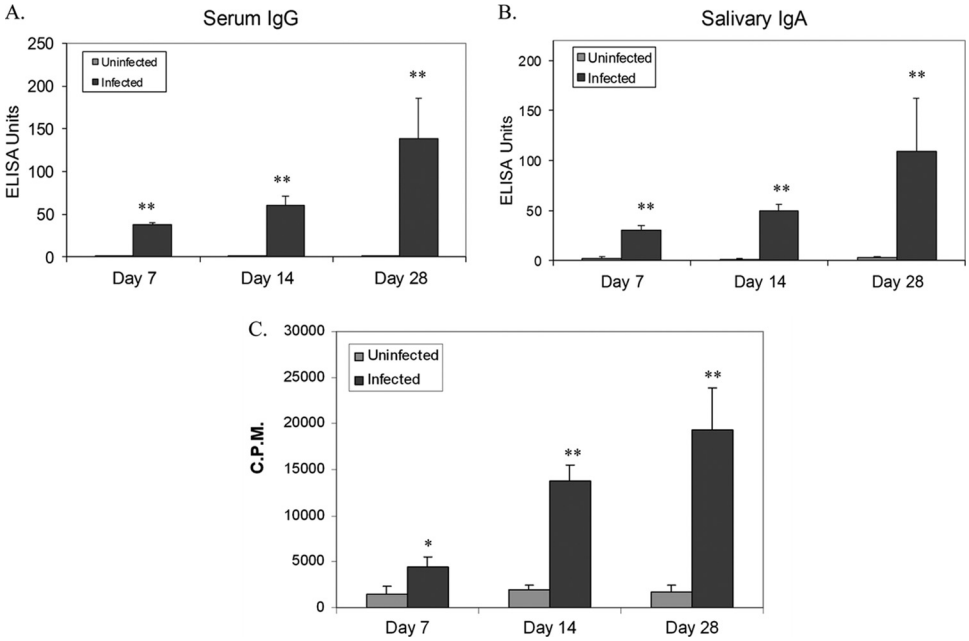

FIG 2 T and B cell responses to *P. gingivalis* after oral infection. Formalin-fixed *P. gingivalis* (10^7 bacteria/well) were coated in duplicate onto 96-well plates. (A) Diluted rat serum (1:500) was applied to the plate, and rabbit anti-rat IgG antibody was added, followed by alkaline phosphatase (ALP)-conjugated goat anti-rabbit IgG antibody. (B) Diluted rat whole saliva (1:20) was applied to the plate, and mouse anti-rat IgA antibody was added, followed by ALP-conjugated goat anti-mouse IgG antibody. Colorimetric reactions were developed with *p*-nitrophenyl phosphate (pNPP) substrate. ELISAs were performed, and measurements are expressed as ELISA units (EU) converted from a standard curve. All readings were recorded with a microplate reader (Bio-Tek Instruments) at 405 nm. **, $P < 0.01$, by a Student *t* test ($n = 6$). (C) Cells from rat cervical lymph nodes (LN) were isolated and cultured in 96-well plates (1×10^4 cells/well) in triplicate in the presence of formalin-fixed *P. gingivalis* (1×10^7 bacteria/well). [^{3}H]thymidine (0.5 μCi/well) was added for the last 16 h of a total of 4-day culture. Samples were harvested onto glass fiber filters, and radioactivity (cpm) was measured in a liquid scintillation spectrometer (PerkinElmer, Waltham, MA). *, $P < 0.05$; **, $P < 0.01$, by a Student *t* test ($n = 6$).

edge of the group designation of the animals, and the recordings were verified by a second examiner. The bone resorption was expressed as total distance between the CEJ and the AvB crest per animal ($n = 6$ for experiment 1, and $n = 4$ for experiment 2).

Tissue preparation and histological TRAP staining. The maxillary samples from each group ($n = 4$ per group) were dissected and fixed in 4% formaldehyde overnight at 4°C. The specimens were then washed consecutively in 5, 10, and 15% glycerol in PBS and decalcified in 10% EDTA–0.1 M Tris for 3 weeks at 4°C. Decalcified samples were cut in half through the midline of the palate, embedded in optimal cutting temperature (OCT) compound (Miles, Elkhart, IN), and frozen at −80°C for 1 h. Serial sections at 6 μm were cut by cryostat sectioning. For TRAP staining, the slides were incubated for 20 to 40 min in the TRAP staining solution at 37°C in the dark until red staining was visible. The slides were then counterstained with hematoxylin. Osteoclasts were identified as multinucleated TRAP-positive cells, lying on the alveolar bone surface. For quantitative image analysis, the number of osteoclasts per millimeter of the alveolar bone surface was measured using an image analysis program (AxioVision; Carl Zeiss MicroImaging Inc., Thornwood, NY).

Quantitative RT-PCR (qRT-PCR). At the termination of experiment 2 (day 28), oral swabs from each rat were resolved in 200 μl of PBS containing protease inhibitor cocktail (Roche). DNA was extracted from each sample as previously described (22) and subjected to real-time PCR (RT-PCR) amplification of the DNA fragment using *P. gingivalis* 16S rRNA gene-specific primers (5′-GAGTTTGATYMTGGCTCAG-3′ and 5′-TCA GTCGCAGTATGGCAA-3′). A universal 16S rRNA gene primer pair was used to quantitate the total bacteria recovered from each animal (5′-GA GTTTGATYMTGGCTCAG and 5′-AAGGAGGTGWTCCARCC-3′). Amplification reactions were carried out in 25 μl of SYBR green reaction mix (Invitrogen) in an iCycler (Bio-Rad) according to the manufacturer's instructions. The quantity of *P. gingivalis* DNA or total bacterial DNA from each sample was extrapolated from the DNA standard curve derived from serial dilution of bacteria with known concentrations. *P. gingivalis* numbers were normalized to the total bacteria count in each sample. Each experiment was carried out in duplicate, and the data were obtained from all animals from each group ($n = 8$).

Statistical analysis. Results obtained from periodontal bone resorption and quantitation of *P. gingivalis* DNA are expressed as means ± standard deviations (SD). Data compiled from T cell proliferation assays, from ELISAs for serum IgG, salivary IgA, and sRANKL, from TRAP staining, and from flow cytometry are expressed as means ± standard errors (SE). A Student's *t* test was used to evaluate significance using the software Excel 2010 (Microsoft). *P* values of ≤0.05 were considered statistically significant.

RESULTS

Serum IgG and salivary IgA antibody response to *P. gingivalis* after oral infection. As expected, after oral infection with *P. gingivalis*, both rat serum IgG and salivary IgA antibodies to *P. gingivalis* were significantly increased at day 7 ($P < 0.01$) and further elevated at day 14 and day 28 compared to the antibody levels in the uninfected animals ($P < 0.01$) (Fig. 2A and B). Proliferation of T cells from cervical lymph nodes (LN) after their exposure to *P. gingivalis* antigen was also greatly increased in infected rats compared to those in the uninfected rats (from 2.5-fold at day 7 to 10-fold at day 28), as detected by ^{3}H incorporation assay (Fig. 2C).

sRANKL detection in rat gingival homogenate. At day 7, there was no difference in soluble RANKL (sRANKL) concentrations in gingival tissues extracted from uninfected and infected rats. However, sRANKL concentrations were significantly higher

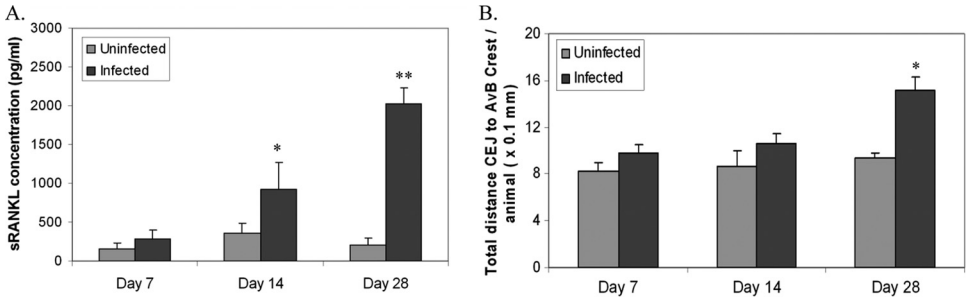

FIG 3 Evaluation of sRANKL production and alveolar bone resorption in rats after *P. gingivalis* infection. (A) sRANKL was detected in rat gingival homogenate by ELISA using a murine sRANKL ELISA development kit (Peprotech). Assays were performed in triplicate. **, $P < 0.01$, by a Student *t* test ($n = 6$). (B) Alveolar bone resorption in rats after *P. gingivalis* infection. Rat maxillae were defleshed, and the distances from the cemento-enamel junction (CEJ) to the alveolar (AvB) crest on the palatal side of each root were measured as described in Materials and Methods. The bone resorption was expressed as the total distance between the CEJ and the AvB crest per animal. *, $P < 0.05$, by a Student *t* test ($n = 6$).

in the gingival homogenates of *P. gingivalis*-infected rats than in those from uninfected rats at both day 14 ($P < 0.05$) and day 28 ($P < 0.01$) (Fig. 3A).

Alveolar bone resorption in rats after *P. gingivalis* infection. The total distances (mm) from the CEJ to the AvB crest of palatal roots were measured to evaluate the level of bone resorption from *P. gingivalis*-infected rats (Fig. 3B). At day 7 and day 14, the total distance from the CEJ to the AvB crest of palatal roots in *P. gingivalis*-infected rats did not differ from that of uninfected rats. However, at day 28, a significant increase in the total distance from the CEJ to the AvB crest of the palatal roots was observed in *P. gingivalis*-infected rats compared to uninfected rats ($P < 0.05$). This increase is in parallel with the increased sRANKL concentrations in the gingivae of *P. gingivalis*-infected rats compared to levels in uninfected rats (Fig. 3A).

Distribution of RANKL-expressing immune cells in rat gingival tissues. The total number of immune cells and the number of RANKL-expressing immune cells in gingival tissues from *P. gingivalis*-infected rats and uninfected controls were determined by flow cytometry at day 28. As expected, all tested cell types (B cells, T cells, natural killer cells, and macrophages) were significantly increased in gingival tissues of *P. gingivalis*-infected rats compared to those in uninfected rats at day 28 ($P < 0.01$), supporting immune cell infiltration of infected gingivae (Fig. 4A). However, only T and B cells, but not natural killer cells and macrophages, demonstrated significantly elevated RANKL expression in the gingival tissues of *P. gingivalis*-infected rats compared to uninfected rats at day 28 ($P < 0.01$) (Fig. 4B).

Inhibition of gingival homogenate-induced TRAP$^+$ cell formation by anti-RANKL IgG. We first evaluated the ability of purified anti-RANKL IgG to affect RANKL-induced osteoclastogenesis of RAW 264.7 cells *in vitro*. After culture for 5 days, the number of TRAP$^+$ multinuclear cells was greatly increased in the presence of recombinant RANKL (rRANKL) compared to the level in the medium-only group. However, such an increase was significantly inhibited by the addition of anti-RANKL IgG (5 μg or 10 μg of anti-RANKL IgG [xRANKL]) in a dose-dependent manner (Fig. 5A, sixth and seventh columns). The anti-RANKL IgG was then used to determine its effect on the inhibition of TRAP$^+$ cell formation induced by gingival homogenate from *P. gingivalis*-infected rats. While the number of TRAP$^+$ cells was greatly increased in the presence of recombinant RANKL (rRANKL) compared to the level in the medium-only group, no changes in the number of TRAP$^+$ cells were observed after removal of rRANKL and subsequent additions of gingival homogenate from uninfected rats at day 28 or of anti-RANKL IgG (Fig. 5B, light bars), indicating that the TRAP$^+$ cell formation is due solely to the initial boost by recombinant RANKL (50 ng/ml). RAW 264.7 cells cultured with 0.25 μg/ml gingival homogenate from *P. gingivalis*-infected rats at day 28 demonstrated an increased number of

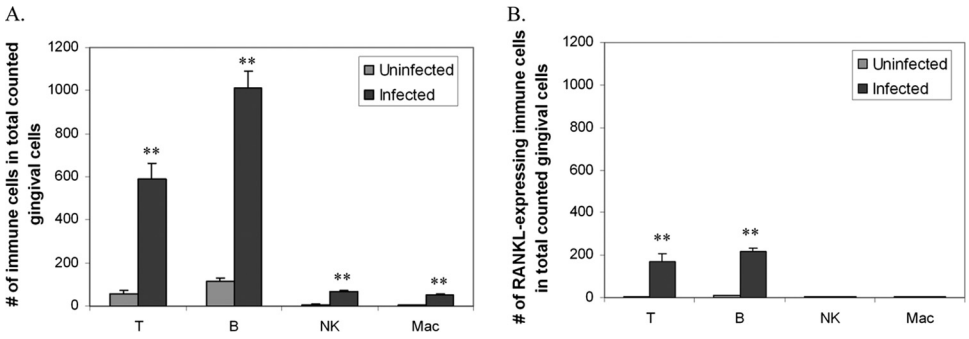

FIG 4 Distribution of RANKL-expressing cells in rat gingival tissues by flow cytometry. On day 28, mononuclear cells from rat gingival tissues were isolated from rat gingival tissues. (A) For cell type distribution, cells were stained with the following monoclonal mouse anti-rat antibodies (Serotec, Oxford, United Kingdom): OX33 (B cells), R73 (T cells), NK-RP1 (natural killer cells) and ED1 (macrophages [MAC]). After cells were washed with PBS, they were stained with FITC-conjugated rat anti-mouse IgG (Jackson ImmunoResearch, West Grove, PA). (B) In some experiments, cells were also stained with rabbit anti-RANKL IgG followed with PE-conjugated goat anti-rabbit IgG (Molecular Probes, Carlsbad, CA). **, $P < 0.01$, by a Student *t* test ($n = 4$).

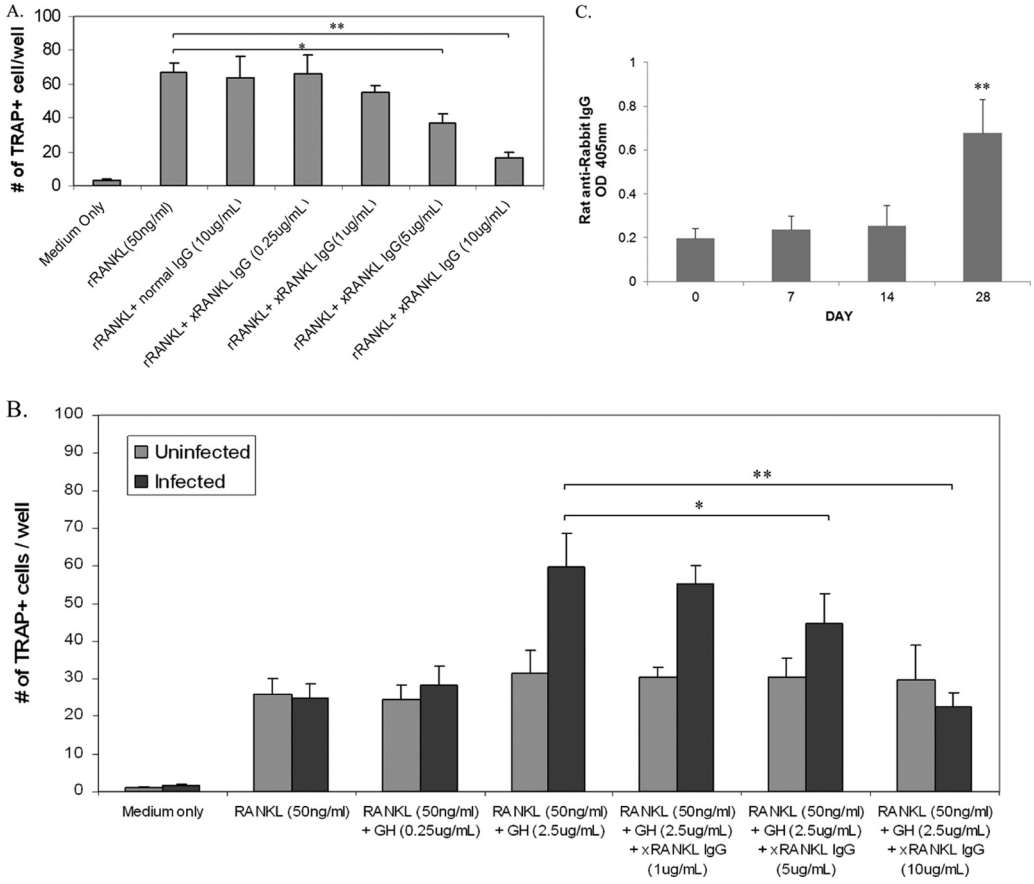

FIG 5 Effect of anti-RANKL IgG on $TRAP^+$ cell formation *in vitro* and serum antibody response *in vivo*. (A) RAW 264.7 cells cultured for 5 days with mrRANKL and rabbit (Rb) normal serum or anti-RANKL IgG. $TRAP^+$ multinuclear cells were counted, and results are expressed as numbers per well in a 96-well plate. (B) RAW 264.7 cells were cultured for 2 days with murine recombinant RANKL (50 ng/ml). Then the medium was replaced with fresh medium without mrRANKL, and cells were cultured with rat gingival homogenates (GH) for another 3 days in the presence or absence of anti-RANKL IgG. $TRAP^+$ multinuclear cells were counted, and results are expressed as numbers per well in a 96-well plate. *, $P < 0.05$; **, $P < 0.01$, by a Student *t* test ($n = 4$). (C) Rat anti-rabbit IgG antibody levels in sera were detected by ELISA on days 0, 7, 14, and 28 after injection of rabbit anti-RANKL IgG (1 μg/site) into the rat palatal gingival papillae. Colorimetric reactions were developed with *p*-nitrophenyl phosphate (pNPP) substrate and measured at 405 nm using a spectrophotometer. Data are presented as means ± SD of 4 sera, each assayed in triplicate. **, $P < 0.01$, by a Student *t* test ($n = 4$). OD, optical density.

$TRAP^+$ cells compared to those from uninfected rats (Fig. 5B, fourth column). The number of gingival homogenate-induced $TRAP^+$ cells was significantly reduced in the presence of anti-RANKL IgG in a dose-dependent manner (Fig. 5B, fifth to seventh columns). This result suggested that osteoclastogenesis induced by gingival tissues from *P. gingivalis*-infected rats is RANKL dependent. We have evaluated the serum antibody responses to rabbit anti-RANKL IgG injected to the animals on days 0, 7, 14, and 28. The results demonstrated that the antibody response to rabbit anti-RANKL IgG could not be detected until at day 28 (Fig. 5C).

Inhibition of periodontal bone resorption after oral infection. As previously demonstrated, a significant increase in the total distance from the CEJ to the AvB crest of palatal roots was observed in *P. gingivalis*-infected rats compared to the distance in uninfected rats at day 28. Gingival injection of anti-RANKL antibody or OPG-Fc (a decoy receptor of RANKL) significantly decreased the total distance compared to the infection-only group (Fig. 6). Such a decrease was not observed with the injection of a nonrelevant human Fc fusion protein, L6-Fc (Fig. 6). Histological TRAP staining demonstrated that gingival injection of anti-

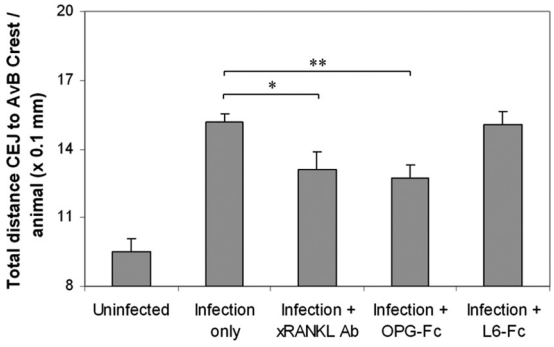

FIG 6 Periodontal bone resorption after oral infection and gingival injections. Rats were divided into 5 groups: group 1, control uninfected; group 2, *P. gingivalis* infection only; group 3, *P. gingivalis* infection with gingival injection of anti-RANKL antibody (1 μg/site); group 4, *P. gingivalis* infection with human OPG-Fc (0.5 μg/site); or group 5, *P. gingivalis* infection with control L6-Fc (0.5 μg/site). After infection, injections were made on the palatal side of maxillae on days 5, 9, and 14. Four weeks after, the maxillae were defleshed, and the distances from the cemento-enamel junction (CEJ) to the alveolar bone (AvB) crest on the palatal side of each root were measured as described in Materials and Methods. Bone resorption was expressed as total distance between the CEJ and the (AvB) crest per animal. Data are expressed as means ± SD (*, $P < 0.05$; **, $P < 0.01$, by a Student *t* test; $n = 4$).

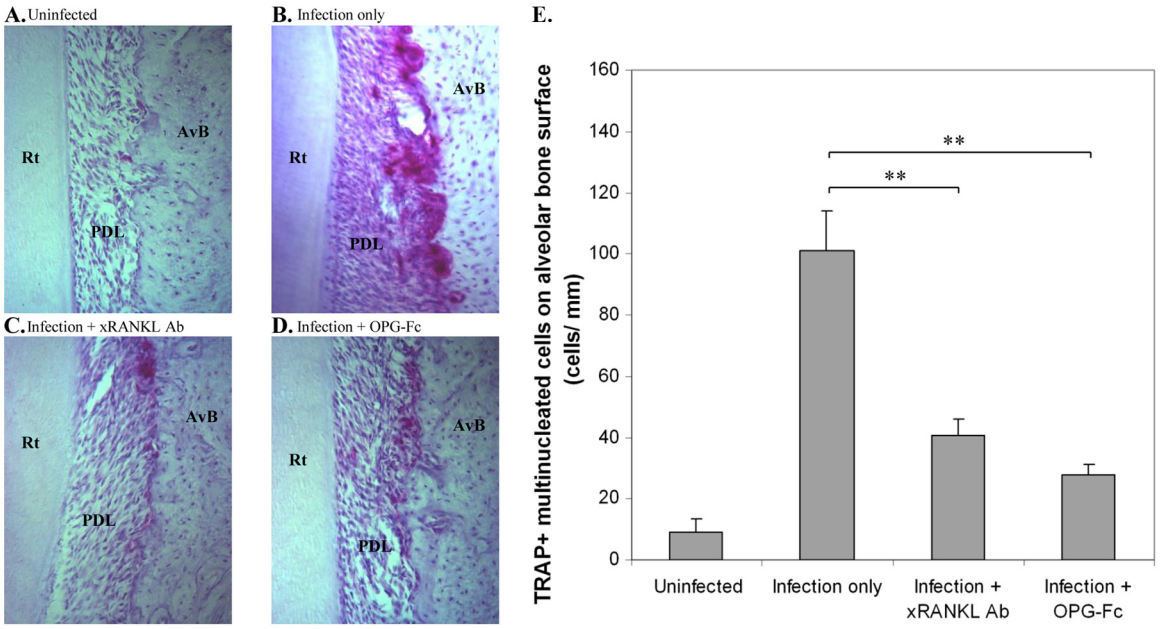

FIG 7 TRAP$^+$ multinucleated cell formation. Four weeks after infection and gingival injection of anti-RANKL antibody or OPG-Fc, rats were sacrificed, and maxillary tissues were sectioned as described in Materials and Methods. TRAP staining was performed to determine the number of multinucleated osteoclast-like cells on the alveolar bone surface. (A) Bone surface of uninfected animal. (B) Bone surface of infected animal without treatment. (C) Bone surface of infected animal injected with anti-RANKL antibody. (D) Bone surface of infected animal injected with OPG-Fc. Rt, root; PDL, periodontal ligament; AvB, alveolar bone. Data are presented as numbers of cells per mm of bone surface (**, $P < 0.01$, by a Student t test; $n = 4$).

RANKL antibody or OPG-Fc significantly reduced *P. gingivalis* infection-associated TRAP$^+$ cell formation along the alveolar bone surface (Fig. 7). This further substantiates that *P. gingivalis* infection-associated osteoclastogenesis in periodontal tissues and the subsequent periodontal bone resorption are RANKL dependent. However, neither anti-RANKL antibody nor OPG-Fc injection reversed the elevated bone resorption and TRAP$^+$ cell formation in *P. gingivalis*-infected rats to levels comparable to those in the uninfected group (Fig. 6 to 7).

Recovery of *P. gingivalis* from rat oral cavities. In order to determine the effect of different treatments on *P. gingivalis* colonization, *P. gingivalis* DNA from rat oral swabs were quantified using real-time PCR, and results were normalized to the total bacterial DNA in the same sample. As expected, *P. gingivalis* DNA was detected from oral swabs of all infected animals at the termination of experiments but was not detected in oral swabs of uninfected rats. Interestingly, injection of anti-RANKL antibody or OPG-Fc in addition to the *P. gingivalis* infection significantly reduced the percentage of *P. gingivalis* relative to the total bacterial count in the rat oral cavity, whereas injection of L6-Fc with *P. gingivalis* infection did not change the percentage of *P. gingivalis* bacteria relative to the total bacterial count in rat oral cavity compared to those rats with infection only (Fig. 8).

DISCUSSION

Current treatment for periodontitis often relies on mechanical procedures and antibiotic administration but lacks strategies directly addressing the immune aspects of the disease. These treatments do not offer complete amelioration of bone resorption accruing around teeth because they do not eliminate the biological causes of periodontal bone resorption (23). The research area "osteoimmunology" has generated considerable interest in the interactions between the immune system and bone (9, 24, 25). Our previous studies have demonstrated the major immune cell contribution to periodontal bone resorption and suggested that excess RANKL shifts the balance of bone metabolism in the direction of catabolism and causes periodontal bone resorption (1, 5). Therefore, an important emphasis of new therapies should involve strategies to treat immune cell-mediated periodontitis.

There have been reports indicating an association between upregulated RANKL levels and the number of *P. gingivalis* bacteria in

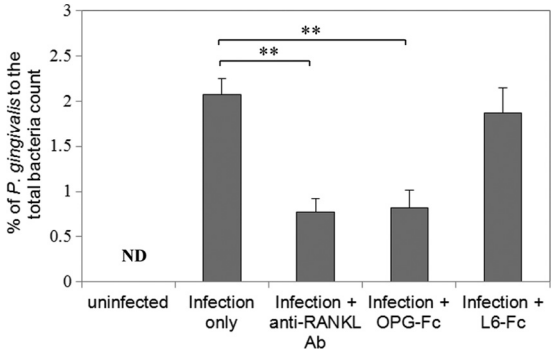

FIG 8 Quantitation of *P. gingivalis* DNA from rat oral cavities. On Day 28, oral swabs from each rat were resolved in 200 μl of PBS containing protease inhibitor cocktail. DNA was extracted from each sample and subjected to real-time PCR amplification of *P. gingivalis*-specific DNA and total bacterial DNA using the following 16S rRNA gene primers: *P. gingivalis*, GAGTTTGATYMTGGC TCAG and TCAGTCGCAGTATGGCAA; universal, 5′-GAGTTTGATYMTG GCTCAG and 5′-AAGGAGGTGWTCCARCC-3′. Data are presented as percentage of *P. gingivalis* bacteria to the total bacterial count in the same sample collected from the oral cavity. **, $P < 0.01$ ($n = 8$ assayed in duplicate); ND, non detectable.

clinically obtained periodontal tissues (26, 27). *P. gingivalis* infection models have been widely used to study immune-mediated periodontal bone resorption (28–30). However, no definitive role of RANKL in *P. gingivalis*-associated periodontal bone resorption has been established. In this study, we have described a rat periodontal infection model that elicits potent host immune responses, immune-mediated RANKL expression, and subsequent periodontal bone resorption. This study suggests that *P. gingivalis* infection-associated periodontal bone resorption is mediated by immune cells in a RANKL-dependent manner. It demonstrates the essential role of RANKL in *P. gingivalis*-associated periodontal bone resorption and can be used as a good model to investigate effects of RANKL-specific intervention regimens during ongoing periodontal infection *in vivo*. It is noted that the injection of anti-RANKL antibody did not bring bone resorption and $TRAP^+$ cell formation back to control levels (Fig. 6 and 7). This could be due to an incomplete RANKL blockage by the time and dosage used for the interventions in this study and/or delayed, neutralizing antibody responses of rats to rabbit anti-RANKL IgG injected into the animals (Fig. 5C). Optimization of time and dosage of the antibody and usage of anti-RANKL F(ab′)2 antibody fragment may potentially improve the efficacy of RANKL blockage and convey better protection.

One of the interesting findings in this study is the reduction of *P. gingivalis* colonization after injection with anti-RANKL antibody or OPG-Fc (Fig. 8). Further studies are warranted to determine the mechanism of such an inhibitory effect toward *P. gingivalis* colonization. One may postulate that inhibition of periodontal bone resorption by anti-RANKL antibody or OPG-Fc generates an unfavorable ecological niche for *P. gingivalis* colonization and could substantially limit bacterial growth. It has been suggested that passive immunization against periodontitis reduces the rate and severity of bone loss, which may temporarily alter the composition of the subgingival microflora (31). This finding is potentially significant since it may indicate that local interference with RANKL-mediated osteoclastogenesis not only ameliorates periodontal bone resorption but may also restrict the niche expansion of the periodontal pathogens. Although outside the scope of the present study, it would be helpful to determine if reduction of *P. gingivalis* colonization affects the numbers of recruited B and T cells or their levels of RANKL expression.

Our recent study using an antigen-specific T cell transfer/gingival antigen injection model demonstrated that anti-RANKL IgG antibody significantly inhibited sRANKL-induced osteoclastogenesis *in vitro* in a dose-dependent manner but also gave rise to a rat antibody response to the rabbit IgG *in vivo*, with no significant inhibition of periodontal bone resorption detected (32). We have evaluated the antibody responses of rats to rabbit anti-RANKL IgG injected into the animals on days 0, 7, 14, and 28, and an antibody response could not be detected until day 28 (Fig. 5C). The two studies are fundamentally different in all aspects of challenge (nature, frequency, and site), anti-RANKL antibody injection schedules (days 5, 9, and 14 in this model versus days −1, 1, and 3 in the T cell transfer/gingival antigen injection model [32]), and experiment duration (28 days in the current model but only 10 days in the transfer model). Why the late onset of such an antibody response to anti-RANKL IgG in the current study did not abolish the observed *in vivo* inhibition of RANKL-induced osteoclastogenesis (Fig. 7) and periodontal bone loss (Fig. 6) by anti-RANKL IgG is not clear, and the underlying mechanism remains to be determined.

The effect of physiological blockade of the RANKL-RANK interaction and the subsequently diminished osteoclastogenesis with OPG-Fc are convincing, but this protein cannot be tested in humans. Studies with the fusion protein OPG-Fc in patients with multiple myeloma were discontinued due to patients developing antibodies to OPG (33). More recent studies have extended this strategy to include immunological blockade of RANKL-RANK interaction using an antibody to RANKL (34, 35). Such a human monoclonal antibody (denosumab, formerly known as AMG 162) has been shown to effectively increase bone mineral density in postmenopausal women and decrease bone resorption (34, 35). Denosumab (trade name of Prolia), has recently been approved by the FDA for women with postmenopausal osteoporosis at increased risk for fractures. Yet serious side effects may occur with denosumab, such as hypocalcemia, infections, and dermatitis, and the long-term effects of denosumab on bone are not known. Therefore, much remains to be determined before such a strategy (blockade of the RANKL-RANK interaction) could be safely and effectively used in the management of bone-resorptive diseases other than osteoporosis. It is conceivable that local immunological blockade of the RANKL-RANK interaction using an antibody to RANKL may be an option for site-specific bone-resorptive diseases such as periodontal disease.

The current study attempted to determine whether live *P. gingivalis* oral infection-induced periodontal bone loss is immune T and B cell-mediated and whether it is RANKL dependent. While *P. gingivalis* infection models have been widely used in research, definitive answers to these questions have not been obtained. Therefore, the current study provides useful information to advance our understanding of *P. gingivalis* infection biology. Our results indicate that a potent systemic T and B cell immune response to *P. gingivalis* can be observed as early as 7 days after infection and is significantly elevated even further at 28 days after infection (Fig. 1). T and B cells could be a major source of RANKL and bone resorption during the immune response to *P. gingivalis* infection (Fig. 2 and 3). Therefore, RANKL inhibition may include reduction of soluble RANKL release or interference with RANKL expression by T/B cells. Interference with these processes should contribute to the abrogation of periodontal bone resorption and prevention of periodontal disease progression. Effects of such interventions may be further studied *in vivo* using this *P. gingivalis* infection-associated periodontal bone resorption model.

ACKNOWLEDGMENTS

The human OPG-Fc fusion protein was kindly provided by Colin Dunstan from Amgen Inc., Thousand Oaks, CA.

This work was supported by NIH grants DE-03420 and DE-07327 from the National Institute of Dental and Craniofacial Research.

REFERENCES

1. **Han X, Kawai T, Eastcott JW, Taubman MA.** 2006. Bacterial-responsive B lymphocytes induce periodontal bone resorption. J. Immunol. **176**:625–631.
2. **Michalek SM, Katz J, Childers NK, Martin M, Balkovetz DF.** 2002. Microbial/host interactions: mechanisms involved in host responses to microbial antigens. Immunol. Res. **26**:223–234.
3. **Taubman MA, Kawai T.** 2001. Involvement of T-lymphocytes in periodontal disease and in direct and indirect induction of bone resorption. Crit. Rev. Oral Biol. Med. **12**:125–135.
4. **Zadeh HH, Nichols FC, Miyasaki KT.** 1999. The role of the cell-mediated

immune response to *Actinobacillus actinomycetemcomitans* and *Porphyromonas gingivalis* in periodontitis. Periodontol 2000 **20**:239–288.
5. **Kawai T, Eisen-Lev R, Seki M, Eastcott JW, Wilson ME, Taubman MA.** 2000. Requirement of B7 costimulation for Th1-mediated inflammatory bone resorption in experimental periodontal disease. J. Immunol. **164**: 2102–2109.
6. **Kawai T, Shimauchi H, Eastcott JW, Smith DJ, Taubman MA.** 1998. Antigen direction of specific T-cell clones into gingival tissues. Immunology **93**:11–19.
7. **Dorner T, Burmester GR.** 2003. The role of B cells in rheumatoid arthritis: mechanisms and therapeutic targets. Curr. Opin. Rheumatol. **15**:246–252.
8. **Fournier C.** 2005. Where do T cells stand in rheumatoid arthritis? Joint Bone Spine **72**:527–532.
9. **Takayanagi H.** 2009. Osteoimmunology and the effects of the immune system on bone. Nat. Rev. Rheumatol. **5**:667–676.
10. **Rogers JE, Li F, Coatney DD, Otremba J, Kriegl JM, Protter TA, Higgins LS, Medicherla S, Kirkwood KL.** 2007. A p38 mitogen-activated protein kinase inhibitor arrests active alveolar bone loss in a rat periodontitis model. J. Periodontol. **78**:1992–1998.
11. **Taubman MA, Valverde P, Han X, Kawai T.** 2005. Immune response: the key to bone resorption in periodontal disease. J. Periodontol. **76**:2033–2041.
12. **Kong YY, Yoshida H, Sarosi I, Tan HL, Timms E, Capparelli C, Morony S, Oliveira-dos-Santos AJ, Van G, Itie A, Khoo W, Wakeham A, Dunstan CR, Lacey DL, Mak TW, Boyle WJ, Penninger JM.** 1999. OPGL is a key regulator of osteoclastogenesis, lymphocyte development and lymph-node organogenesis. Nature **397**:315–323.
13. **Lacey DL, Timms E, Tan HL, Kelley MJ, Dunstan CR, Burgess T, Elliott R, Colombero A, Elliott G, Scully S, Hsu H, Sullivan J, Hawkins N, Davy E, Capparelli C, Eli A, Qian YX, Kaufman S, Sarosi I, Shalhoub V, Senaldi G, Guo J, Delaney J, Boyle WJ.** 1998. Osteoprotegerin ligand is a cytokine that regulates osteoclast differentiation and activation. Cell **93**:165–176.
14. **Udagawa N, Takahashi N, Jimi E, Matsuzaki K, Tsurukai T, Itoh K, Nakagawa N, Yasuda H, Goto M, Tsuda E, Higashio K, Gillespie MT, Martin TJ, Suda T.** 1999. Osteoblasts/stromal cells stimulate osteoclast activation through expression of osteoclast differentiation factor/RANKL but not macrophage colony-stimulating factor. Bone **25**:517–523.
15. **Kong YY, Boyle WJ, Penninger JM.** 1999. Osteoprotegerin ligand: a common link between osteoclastogenesis, lymph node formation and lymphocyte development. Immunol. Cell Biol. **77**:188–193.
16. **Toraldo G, Roggia C, Qian WP, Pacifici R, Weitzmann MN.** 2003. IL-7 induces bone loss in vivo by induction of receptor activator of nuclear factor kappa B ligand and tumor necrosis factor alpha from T cells. Proc. Natl. Acad. Sci. U. S. A. **100**:125–130.
17. **Wyzga N, Varghese S, Wikel S, Canalis E, Sylvester FA.** 2004. Effects of activated T cells on osteoclastogenesis depend on how they are activated. Bone **35**:614–620.
18. **Kawai T, Matsuyama T, Hosokawa Y, Makihira S, Seki M, Karimbux NY, Goncalves RB, Valverde P, Dibart S, Li YP, Miranda LA, Ernst CW, Izumi Y, Taubman MA.** 2006. B and T lymphocytes are the primary sources of RANKL in the bone resorptive lesion of periodontal disease. Am. J. Pathol. **169**:987–998.
19. **Valverde P, Kawai T, Taubman MA.** 2004. Selective blockade of voltage-gated potassium channels reduces inflammatory bone resorption in experimental periodontal disease. J. Bone Miner. Res. **19**:155–164.
20. **Teng YT, Nguyen H, Gao X, Kong YY, Gorczynski RM, Singh B, Ellen RP, Penninger JM.** 2000. Functional human T-cell immunity and osteoprotegerin ligand control alveolar bone destruction in periodontal infection. J. Clin. Invest. **106**:R59–67.
21. **Theill LE, Boyle WJ, Penninger JM.** 2002. RANK-L and RANK: T cells, bone loss, and mammalian evolution. Annu. Rev. Immunol. **20**:795–823.
22. **Taubman MA, Kawai T, Han X.** 2007. The new concept of periodontal disease pathogenesis requires new and novel therapeutic strategies. J. Clin. Periodontol. **34**:367–369.
23. **Cochran DL.** 2008. Inflammation and bone loss in periodontal disease. J. Periodontol. **79**:1569–1576.
24. **Lorenzo J, Horowitz M, Choi Y.** 2008. Osteoimmunology: interactions of the bone and immune system. Endocr. Rev. **29**:403–440.
25. **Walsh MC, Kim N, Kadono Y, Rho J, Lee SY, Lorenzo J, Choi Y.** 2006. Osteoimmunology: interplay between the immune system and bone metabolism. Annu. Rev. Immunol. **24**:33–63.
26. **Sakellari D, Menti S, Konstantinidis A.** 2008. Free soluble receptor activator of nuclear factor-κB ligand in gingival crevicular fluid correlates with distinct pathogens in periodontitis patients. J. Clin. Periodontol. **35**: 938–943.
27. **Wara-aswapati, N, Surarit R, Chayasadom A, Boch JA, Pitiphat W.** 2007. RANKL upregulation associated with periodontitis and *Porphyromonas gingivalis*. J. Periodontol. **78**:1062–1069.
28. **Baker PJ, Evans RT, Roopenian DC.** 1994. Oral infection with *Porphyromonas gingivalis* and induced alveolar bone loss in immunocompetent and severe combined immunodeficient mice. Arch. Oral Biol. **39**:1035–1040.
29. **Gibson FC, III, Genco CA.** 2001. Prevention of *Porphyromonas gingivalis*-induced oral bone loss following immunization with gingipain R1. Infect. Immun. **69**:7959–7963.
30. **Liang S, Krauss JL, Domon H, McIntosh ML, Hosur KB, Qu H, Li F, Tzekou A, Lambris JD, Hajishengallis G.** 2011. The C5a receptor impairs IL-12-dependent clearance of *Porphyromonas gingivalis* and is required for induction of periodontal bone loss. J. Immunol. **186**:869–877.
31. **Persson GR.** 2005. Immune responses and vaccination against periodontal infections. J. Clin. Periodontol **32**(Suppl 6):39–53.
32. **Lin X, Han X, Kawai T, Taubman MA.** 2011. Antibody to receptor activator of NF-κB ligand ameliorates T cell-mediated periodontal bone resorption. Infect. Immun. **79**:911–917.
33. **Khosla S.** 2005. Magic bullets to kill nasty osteoclasts. Endocrinology **146**:3233–3234.
34. **Lewiecki EM, Miller PD, McClung MR, Cohen SB, Bolognese MA, Liu Y, Wang A, Siddhanti S, Fitzpatrick LA.** 2007. Two-year treatment with denosumab (AMG 162) in a randomized phase 2 study of postmenopausal women with low BMD. J. Bone Miner. Res. **22**:1832–1841.
35. **McClung MR, Lewiecki EM, Cohen SB, Bolognese MA, Woodson GC, Moffett AH, Peacock M, Miller PD, Lederman SN, Chesnut CH, Lain D, Kivitz AJ, Holloway DL, Zhang C, Peterson MC, Bekker PJ.** 2006. Denosumab in postmenopausal women with low bone mineral density. N. Engl. J. Med. **354**:821–831.